Journal of Applied Electrochemistry **30**: 1439–1444, 2000.

Effects of baffle length on mass transfer in a parallel plate rectangular electrochemical cell†

C.F. ODUOZA and A.A. WRAGG
School of Engineering and Computer Science, Exeter University, Exeter, EX4 4QF, Great Britain

Received 30 March 2000; accepted in revised form 30 June 2000

Key words: baffle length, electrochemical cell, mass transfer, parallel plate

Abstract

Global mass transfer measurements in unbaffled and baffled configurations using different baffle lengths and Reynolds numbers have been made in a parallel plate cell of rectangular geometry. The entry jet arrangement and the repeated 180° changes in direction of the flow, followed by the exit, produces extremely complex hydrodynamics in the cell. A plot of mass transfer coefficient against baffle length shows an increase in mass transfer with baffle length. Comparison of data for the present work with those of other workers for similar devices showed higher mass transfer due to the modifications incorporated in the present cell.

List of symbols

A	electrode surface area (m^2)
C	bulk species concentration (mol m^{-3})
D	diffusion coefficient (m^2 s^{-1})
d_e	duct equivalent diameter, $\frac{2ws}{w+s}$ (m)
F	faradaic constant (96 487 C mol^{-1})
I_L	limiting electrolysis current (A)
K	mass transfer coefficient (m s^{-1})
L	electrode length (m)
Re	Reynolds number ($d_e v\ \rho/\mu$)
s	interelectrode distance
Sc	Schmidt number (v/D)
Sh_{de}	Sherwood number based on cell or channel equivalent diameter (Kd_e/D)
w	width of cell or cell channel
z	electrons exchanged in electrode reaction
v	mean fluid velocity in cell or cell channel (m s^{-1})

Greek letters

ρ	fluid density (kg m^{-3})
ν	kinematic viscosity (m^2 s^{-1})
μ	dynamic viscosity (kg s^{-1} m^{-1})

1. Introduction

Many electrochemical processes are operated under limiting or near limiting current conditions to maximise the space time yield of the electrolyser. Mass transport, therefore, determines the rate of conversion of reactant to product and it is common to use inert turbulence promoters, baffles, and/or high fluid velocity to enhance the mass transport to the electrode surface and, hence, the cell current density.

The relationship between a parallel plate cell geometry, the cell flow conditions and mass transfer performance has recently been described for some specific cases [1, 2]. The aim of such studies is to enhance reactor performance and to obtain a greater understanding of the physical phenomena involved. Goodridge and coworkers [3, 4] had earlier worked with both small and large models of baffled parallel plate cells with segmented electrodes.

This paper describes measurements carried out in a cell of rectangular geometry, with entry configuration, provision for baffles and dimensions such that three-dimensional fluid flow distribution effects are encountered. The entry configuration is initially a two-dimensional jet, but the flow develops three dimensionally due to the complex geometry of the cell. By placing baffles in the frame of the cell, a serpentine flow path is also created. Wragg and Leontaritis [5, 6] have previously described a cell of similar configuration. Their local mass transfer coefficient values given by arrays of surface-flush mounted nickel minielectrodes exhibited a distribution that reflected the complex hydrodynamics associated with phenomena such as cell inlet and exit effects and flow reversal at the baffles. However, the basic difference between their design and that for the present work lies in the entry and exit

† Dedicated to the memory of Daniel Simonsson

configurations as well as in the design of the baffles. The present configuration was decided to simplify the cell geometry and facilitate a parallel programme of numerical modelling in the context of a collaborative project [7]. In particular, this work describes a study of the effect of baffle length on overall mass transfer performance. Goodridge and Mamoor [3] have also studied mass transfer in baffled electrolytic cells with similar dimensions as in the present work.

2. Experimental details

The cell, which was mounted horizontally, was made up of a flat plate cathode and anode and a frame made in grey PVC. The baffles, also fabricated in PVC, were 5 mm thick and occupied the full height of the cell. Figure 1 shows a plan view of the cell showing the frame and a plate (dimensions in mm). The cathodes and the anodes were made of 3 mm nickel sheet, 150 mm long and 150 mm wide, the nominal active area being 0.0225 m^2. The interelectrode gap was 15 mm, this being set by the frame thickness. This work employed square cut PVC baffles of different lengths whereas those of Wragg and Leontaritis [5, 6] and Goodridge and Mamoor [3] were full length with lozenge shaped openings near their ends. Again, while the entry and exit slots in this cell were rectangular shaped, those of the previous workers [3, 5, 6] were three holes each of 5 mm diameter.

Baffle lengths measuring 20, 52.5, 75, 97.5, 112.5 and 125 mm were used for this work and their effects on global mass transfer rate were determined. Mass transfer measurements were also carried out in an unbaffled configuration for comparison.

The rig carrying the parallel plate cell consisted of a 100 dm^3 reservoir, equipped with a cooling coil, a Beresford PV 121 chemical pump and a rotameter covering a flow rate range of 5–220 L min^{-1}. Oxygen-free nitrogen was provided to condition the electrolyte. It was possible to regulate the electrolyte temperature in the reservoir by means of heat exchangers supplied with a mixture of cold and hot tap water.

Table 1. Physical properties of the electrolyte at 20 °C

Density	1020.5 kg m^{-3}
Viscosity	1.105×10^{-3} kg m^{-1} s^{-1}
Diffusivity of ferricyanide ion	6.631×10^{-10} m^2 s^{-1}
Schmidt number	1633

The electrolyte was an aqueous solution of 0.005 M potassium ferricyanide, 0.01 M potassium ferrocyanide and 0.5 M sodium hydroxide ($K_3Fe(CN)_6/K_4Fe(CN)_6$/NaOH–H_2O). The ferrocyanide concentration was double the ferricyanide concentration to ensure a limiting reaction rate at the cathode. The electrolyte was prepared using distilled water and AR grade reagents. 50 L of solution was usually prepared for each run. The physical properties of the electrolyte are shown in Table 1 [5].

The electrolyte is easily decomposed in the presence of light to hydrogen cyanide which both poisons the electrode and alters the concentration. The solution was therefore analysed frequently to determine its concentration by UV spectrophotometry at a wavelength of 419 nm.

The reactions in this system are as follows:

$$Fe(CN)_6^{3-} + e^- \longrightarrow Fe(CN)_6^{4-} \quad \text{at the cathode}$$

$$Fe(CN)_6^{4-} \longrightarrow Fe(CN)_6^{3-} + e^- \quad \text{at the anode}$$

The well known limiting diffusion current technique as applied in several other applications [8, 9] was used for the mass transfer measurements and cathodic mass transfer coefficients were determined from the well defined limiting currents in the plateau regions of the

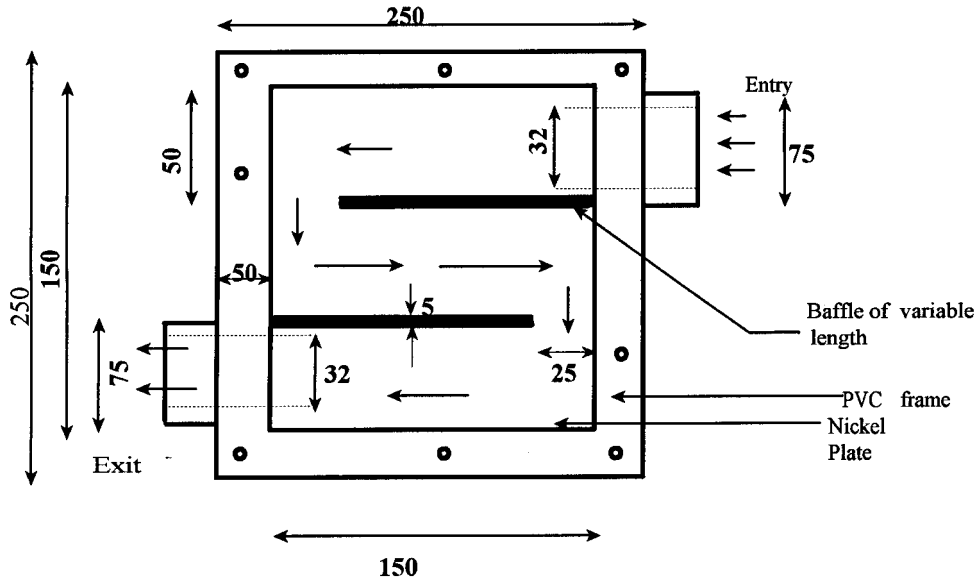

Fig. 1. Planar view of parallel plate cell showing frame and plate.

current–voltage curves. Measurements of mass transfer coefficients were made for a wide range of flow rates and the full range of baffle lengths available. Data were also obtained in the absence of any baffling.

The equation

$$K = \frac{I_L}{zFAc_\infty} \tag{1}$$

was used to calculate mass transfer coefficients from the limiting current values.

3. Results and discussion

Polarization data for the cell in the unbaffled configuration at different cell Reynolds numbers are shown in Figure 2. Well-defined plateaux were obtained at all flow rates allowing mass transfer coefficients to be calculated (Equation 1). Figure 3 shows the plot of mass transfer coefficient against flow rate in the unbaffled configurations, and for baffles of length 125 mm, the longest used. Distinctly higher limiting currents were obtained in the baffled configuration at identical volumetric flow rates due to increased local flow velocity in the presence of baffles and the more efficient utilisation of the electrode surface.

Figures 4 and 5 show plots of Sherwood number against Reynolds number for the unbaffled case and the cell with 125 mm baffles, respectively. The equations describing the plots are as follows:

$$Sh = 0.49\,Re^{0.70}Sc^{0.33} \tag{2}$$

for the unbaffled cell and in the range Re = 900–10 000

$$Sh = 0.91\,Re^{0.6}Sc^{0.33} \tag{3}$$

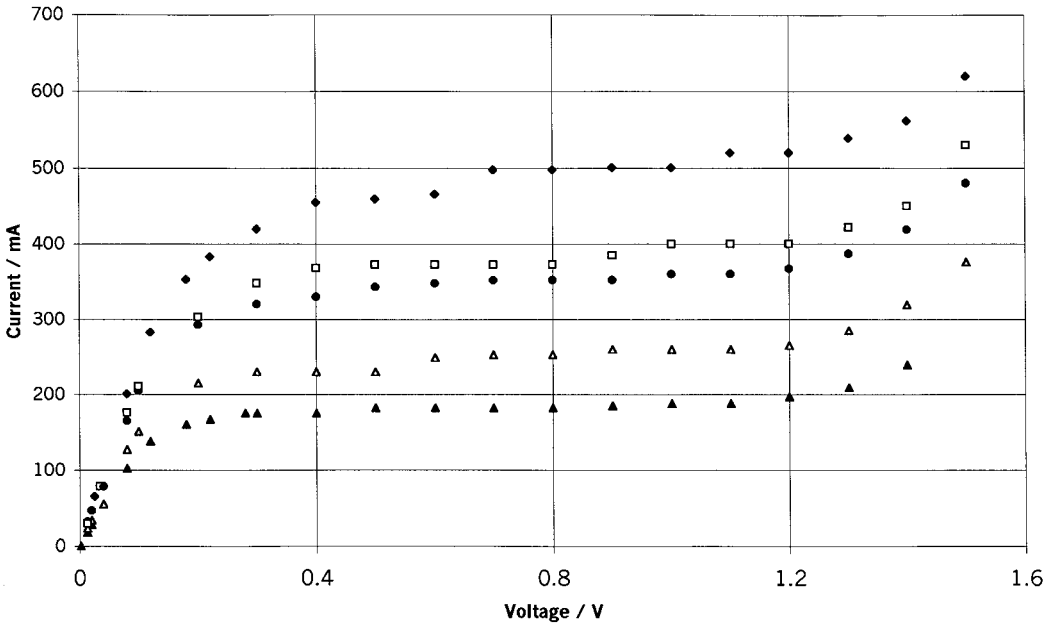

Fig. 2. Polarization data for unbaffled cell at different cell Reynolds numbers. Key for *Re*: (▲) 934, (△) 1500, (●) 3200, (□) 4480 and (◆) 7190.

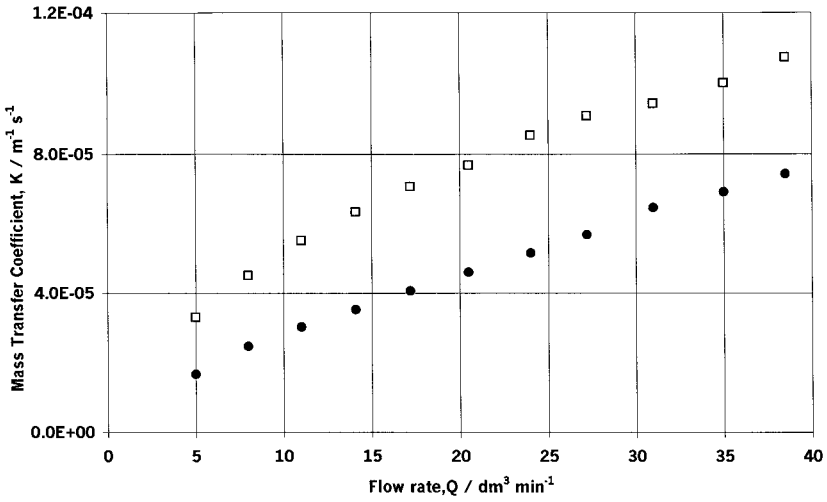

Fig. 3. Plot of mass transfer coefficient against flow rate for baffled and unbaffled cell. Key: (□) baffled and (●) unbaffled.

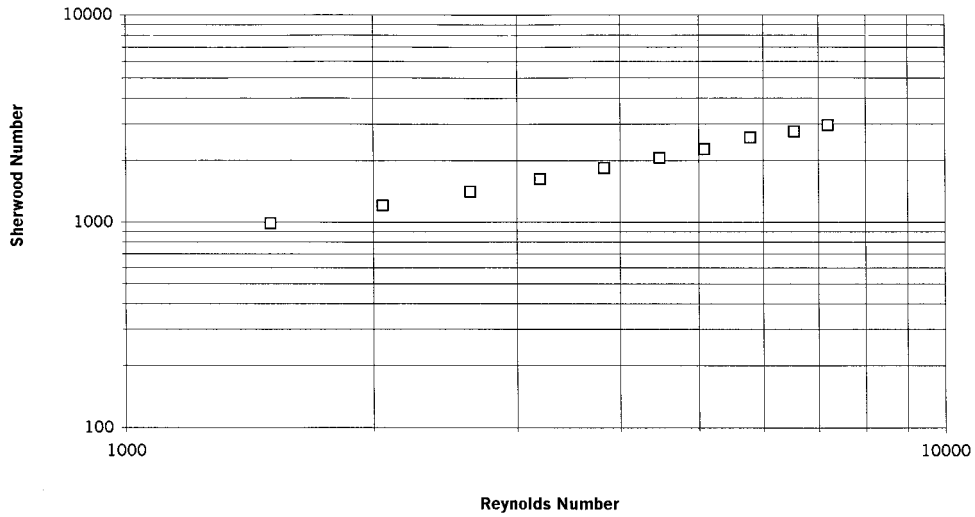

Fig. 4. Plot of Sherwood number against Reynolds number for the unbaffled cell.

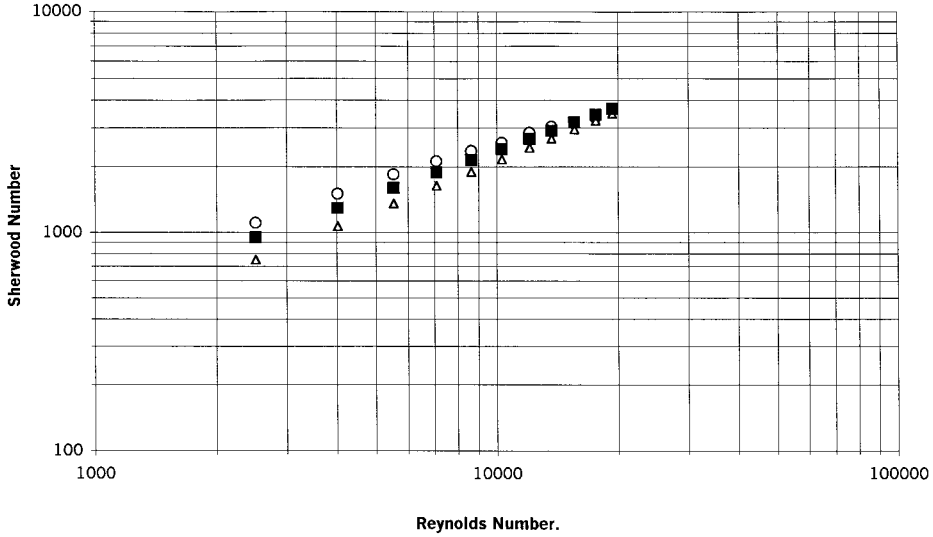

Fig. 5. Comparative plot of Sherwood number against Reynolds number for baffled cells. Key: (○) present work, (△) Wragg and Leontaritis [5] and (■) Goodridge and Mamoor [3].

for the baffled configuration in the range Re = 2500–20 000.

Figure 5 also shows a comparison of the present data (only plotted in the same range as those of other workers) for the 125 mm baffled cell with those of Goodridge and Mamoor [3] and Wragg and Leontaritis [5]. Generally good agreement is observed but data obtained in the present work are higher than those of the previous workers. This is attributable to the distinctive jet inlet characteristics and the square cut baffles in the present cell giving greater hydrodynamic efficiency.

A plot of mass transfer coefficient against flow rate for all the different baffle lengths is shown in Figure 6. Mass transfer increases with increase in baffle length at all flow rates. The unbaffled configuration gives the lowest mass transfer while the longest baffle length of 125 mm gives the highest values. Figure 7 shows a plot of mass transfer coefficient against baffle length at different flow rates. Mass transfer coefficient is seen to increase with baffle length for all flow rates; the longer the baffle, the more effective the flow distribution over the electrode surface. It is clear that K is still increasing strongly with baffle length even at long lengths. It would be of interest to investigate to what extent this trend continued as the baffle length approached the full length of the cell. The penalty of increased cell pressure drop would, of course, become an important consideration.

Comparison of data for selected different baffle lengths with those of Wragg and Leontaritis using full length baffles with lozenge shaped openings and obtained in the high Re range is shown as a plot of Sh against Re in Figure 8. Data obtained from the present work showed marginally higher mass transfer values for the longest baffles. Figure 8 also includes data for lower flow rates, that is, Reynolds numbers less than 200.

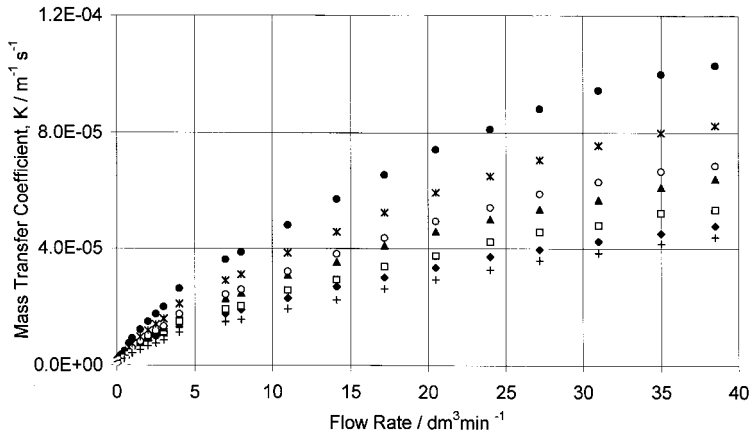

Fig. 6. Plot of mass transfer coefficient against flow rate at different baffle lengths. Key: (◆) 30, (□) 52.5, (▲) 75, (○) 97.5, (□) 112 and (●) 125 mm. (+) Unbaffled.

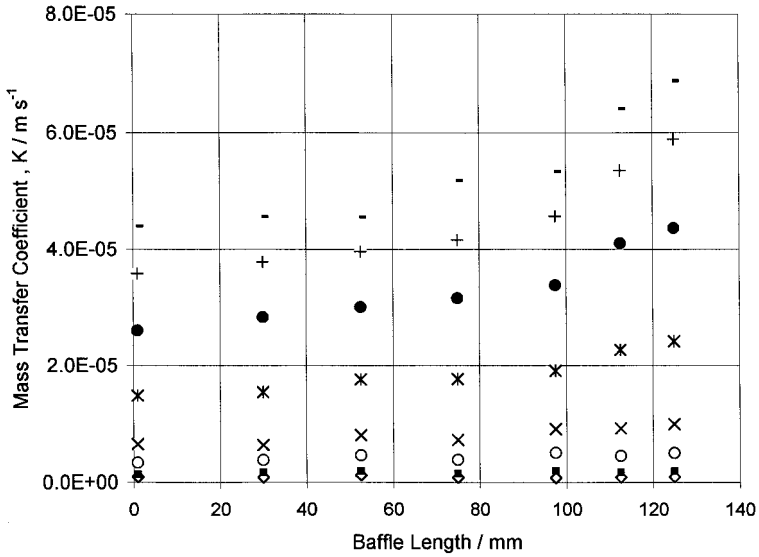

Fig. 7. Plot of mass transfer coefficient against baffle length at different flow rates. Key: (◇) 0.02, (■) 0.2, (○) 0.8, (×) 2, (✱) 7, (●) 17.2, (+) 27.2 and (−) 38.5 L min^{-1}.

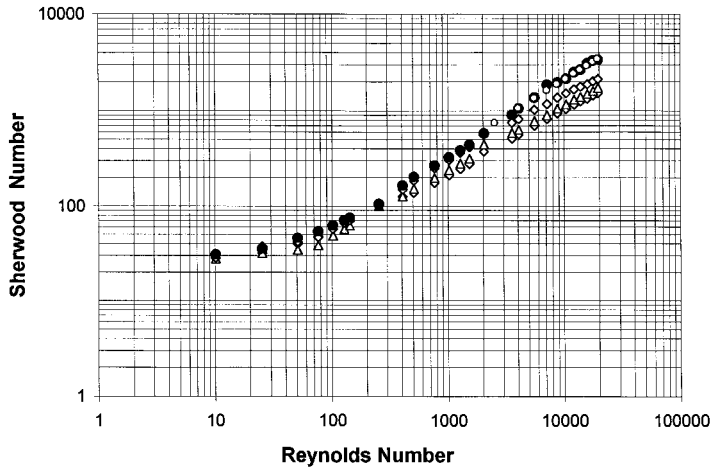

Fig. 8. Plot of Sherwood number against Reynolds number for selected baffle lengths. Key: (□) 30, (△) 75, (◆) 112.5 and (●) 125 mm. (○) Wragg and Leontaritis [5].

It can be seen that these deviate from the straight line plots of the higher *Re* data and asymptote towards a natural convection limit as has been shown for combined convection problems in other types of cell [10].

4. Conclusion

The results demonstrate the mass transfer enhancing effect of a baffled configuration compared to an unbaffled cell. They also confirm that the longer the baffle length the higher the global mass transfer rate. The work has also demonstrated the superior effect of the rectangular entry and exit configurations combined with the square cut baffles over that of the three jets and the lozenge shaped baffle openings used in previous work.

Acknowledgement

This work was performed under Brite–Euram III contract number: BRPR-CT95-0008.

References

1. W.M. Taama, R.E. Plimley and K. Scott, Mass transfer rates in a DEM electrochemical cell, *Proceedings of the 4th European Symposium on Electrochemical Engineering (CHISA)*, Institute of Chemical Technology, Prague (1996), pp. 289–295.
2. D.A. Szanto, P. Trinidad, I. Whyte and F.C. Walsh, Electrosynthesis and mass transport measurements in laboratory filter-press reactor, *Proceedings of the 4th European Symposium on Electrochemical Engineering (CHISA)*, Institute of Chemical Technology, Prague (1996), pp. 273–280.
3. F. Goodridge, G.M. Mamoor and R.E Plimley, *IChemE Symposium Series* No. **98** (1985) 61.
4. G.M. Mamoor, PhD thesis, University of Newcastle-on-Tyne, UK (1983).
5. A.A. Wragg and A.A. Leontaritis, *Chem. Eng. J.* **66** (1997) 110.
6 A.A. Wragg and A.A. Leontaritis, *Dechema Monographs* **123** (1990) 345.
7. C.F. Oduoza and A.A. Wragg, Development and evaluation of methods for the prediction of current density and layer thickness distribution in electrochemical cells, Final report of Brite–Euram III, contract number: BRPR-CT95-0008 (1995–1998).
8. D.J Tagg, M.A. Patrick and A.A. Wragg, *Trans. I. Chem. Eng.* **57** (1979) 176.
9. A.A. Wragg, D.J. Tagg and M.A. Patrick, *J. Appl. Electrochem.* **10** (1989) 43.
10. C.F. Oduoza and A.A. Wragg, *J. Appl. Electrochem.* **28** (1998) 697.